Economic optimization of coastal flood defence systems including storm surge barrier closure reliability

Mooyaart, Leslie F.; Bakker, Alexander M.R.; van den Bogaard, Johan A.; Rijcken, Ties; Jonkman, Bas

Important note
To cite this publication, please use the final published version (if applicable).
Please check the document version above.

ORIGINAL ARTICLE

CIWEM Chartered Institution of Water and Environmental Management   Journal of Flood Risk Management   WILEY

Economic optimization of coastal flood defence systems including storm surge barrier closure reliability

Leslie F. Mooyaart[1,2] | Alexander M. R. Bakker[1,2] | Johan A. van den Bogaard[3] | Ties Rijcken[1] | Bas Jonkman[1,4]

[1]Department of Hydraulic Engineering, Delft University of Technology, Delft, The Netherlands

[2]Department of Storm Surge Barriers and Guard Locks, Rijkswaterstaat, The Netherlands

[3]Department of Water Barriers, Rijkswaterstaat, The Netherlands

[4]Texas A&M Galveston, Texas, USA

Correspondence
Leslie F. Mooyaart, Department of Hydraulic Engineering, Delft University of Technology, Delft, The Netherlands.
Email: l.f.mooyaart@tudelft.nl

Funding information
Directorate General of Public works and Water Management (Rijkswaterstaat), the Netherlands

Abstract

Storm surge barriers are large movable hydraulic structures which close during a storm surge to prevent coastal floods. In the regions they protect, a failure to close the barrier is often the most likely cause for a catastrophic flood. Nevertheless, flood risk assessments usually only focus on raising flood defences behind the barrier. Despite its importance, there is no general method to assess the costs and benefits of improving the closure reliability. This paper presents a model that optimises investments considering both closure reliability improvements and raising flood defences behind the barrier, using the region protected by the Maeslant barrier as a case. We substantiate that constructing the Maeslant barrier was an optimal economic decision. Moreover, we demonstrate large investments such as a redundant barrier already being economically sound with a few decimetres of sea level rise. Based on our experience with this case study, we expect the model is useful in finding strategies to adapt to rising sea levels and other developments that cause coastal flood risk to rise worldwide.

KEYWORDS

economic optimization, flood defence, flood risk, reliability, storm surge barrier

1 | INTRODUCTION

A storm surge barrier is a fully or partly movable barrier that is closed temporarily to limit water levels in the basin behind the barrier preventing flooding of the area surrounding the inner basin. The barrier is kept open during normal conditions to allow for tidal exchange and unhindered navigation (Mooyaart & Jonkman, 2017). As a result of these characteristics, storm surge barriers incorporate advanced technology for their operation, such as sophisticated weather and water level forecast models. Moreover, they involve relatively high cost,

typically a hundred million to several billion euros of investment and millions of euros for maintenance annually.

Coastal flood risk is rising due to several factors. Climate change raises sea levels and affects storminess and river flow (Calafat et al., 2022). Moreover, growing populations, growing value of assets, and subsidence increase the vulnerability of coastal zones. To maintain coastal flood risk at an acceptable level, coastal areas need to adapt (Hallegatte et al., 2013).

At a coastal defence system with a storm surge barrier, there are a number of coastal flood risks. The storm

surge barrier can (1) fail to close, (2) fail to open, (3) overflow and overtop, (4) fail structurally. Moreover, precipitation, river discharge or internal wind set-up can raise water levels of the inner basin even with a successful barrier closure. Yet, at four out of the five regions protected by Dutch storm surge barriers, the risk of a failure to close is the largest (Maeslant barrier [HKV, 2006]; Hollandsche IJssel barrier [Vader et al., 2022]) or the second largest (Eastern Scheldt barrier [Rijkswaterstaat, 2008], Ramspol [Rijkswaterstaat, 2002]). Therefore, we expect that the risk of a failure to close, that is, the lack of closure reliability, is important for storm surge barriers outside the Netherlands as well.

Closure reliability is defined as the probability of a storm surge barrier to close when required. A coastal flood occurs if both the storm surge barrier fails to close and secondary protection behind the barrier collapses. Many technical components, such as operating mechanisms, drives, switchboards, and computers, but also the reliability of operating and maintenance staff, affect the ability to close (Lewin et al., 2003). Although individual components are often highly reliable, the number of components and maintenance and operation actions can accumulate to probabilities of failed closures around 1:100 on demand (Maeslant & Eastern Scheldt barrier).

Although relevant, current economic decision-making models do not include closure reliability. Most recent developments in coastal flood risk decision-making focus on the effect of uncertainty or robustness of measures (Haasnoot et al., 2013; Kim et al., 2019; Ruig et al., 2019; van der Pol et al., 2021). Groves and Sharon (2013) explore a wide range of flood risk reduction measures, and Aerts et al. (2014) even include storm surge barriers, but they do not consider improving closure reliability. Kind (2014) and Eijgenraam et al. (2017) built upon the well-known Van Dantzig model, balancing dike raise cost and coastal flood risk. These models are, however, only suitable for optimising a single flood defence. As a failure to close a storm surge barrier can only lead to coastal floods if secondary flood protection fails as well, an economic decision-making model is required which can handle double barrier systems. The CPB Netherlands Bureau for Economic Policy Analysis (2013) and Dupuits et al. (2017) address these types of systems. However, they only consider structural and overtopping failure modes, which are often not dominant for coastal flood defence systems with storm surge barriers. Consequently, no economic optimization models are available which include closure reliability as a parameter.

This paper presents an economic optimization model for a coastal flood defence system with a storm surge barrier, which takes closure reliability into account. We choose to include closure reliability into the simple, but widely used economic optimization model of van Dantzig (1956) for two reasons: First, the model of van Dantzig is analytical and, therefore, relatively simple. As Vezér et al. (2018) indicate, simple economic decision-making models are better affordable, more transparent, and more amenable to reproducibility and scrutiny. Moreover, simpler models can assess a wider range of options and scenarios, as van Berchum et al. (2019, 2020) and Ceres et al. (2019, 2022) promote. They also help in policy-making preceding more detailed analyses supporting the final investments. Second, the model optimises dike raise, which is still a popular flood risk reduction measure in the Netherlands. Other measures such as improving evacuation or raising hinterland are considered, but are not applied. Figure 1 indicates the principle of the model of van Dantzig (1956) and how closure reliability is added to this model.

The model is applied to the region protected by the Maeslant barrier (Rotterdam, the Netherlands), which is presented in Section 3. Section 4 shows the results of the optimization, where the effect of sea level rise is also explored. Section 5 discusses the model, followed by concluding remarks in Section 6.

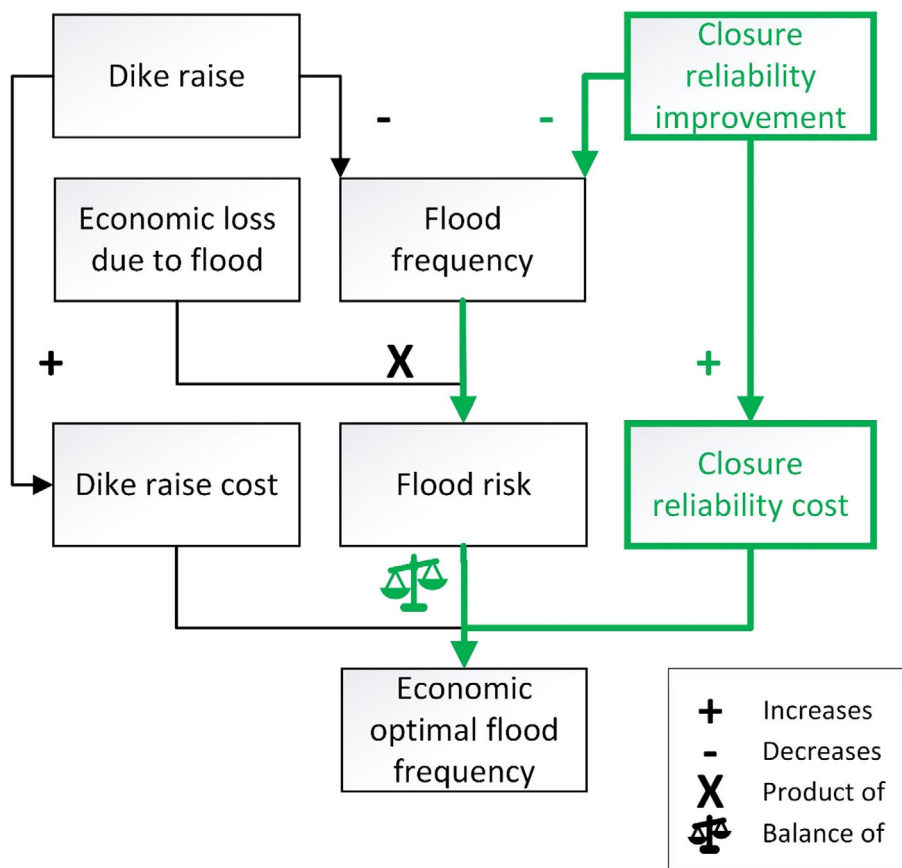## 2 | OPTIMIZATION MODEL

2.1 | Optimization problem

In this optimization problem, we look into investments in closure reliability (C_{SSB}) and/or raising polder dikes behind the barrier (C_D). Investments in both measures reduce flood frequency in the polder and, thus, lower coastal flood risk. Here, coastal flood risk is expressed as the present value of expected damage over the considered lifetime R (M€). The economic optimal solution has the lowest total cost TC (M€), that is, the lowest sum of investment cost and expected damage:

$$\min(TC) = \min(C_{SSB} + C_D + R). \quad (1)$$

2.2 | Flood frequency

Figure 2 presents a schematic top view of the basic coastal defence system considered in this paper. Figure 3 shows the corresponding schematic cross-section. As these figures indicate, both the storm surge barrier and the dike need to fail before a coastal flood takes place. We consider these two failure events to be independent of each other. Hence, the flood frequency F_f (per year) is

FIGURE 1 Process to find economic optimal flood frequencies. In black, the principle of the model of van Dantzig (1956) is shown. In green, the addition proposed by this paper is indicated.

FIGURE 2 Schematic overview of a storm surge barrier flood protection system with one polder considered for the economic optimization model.
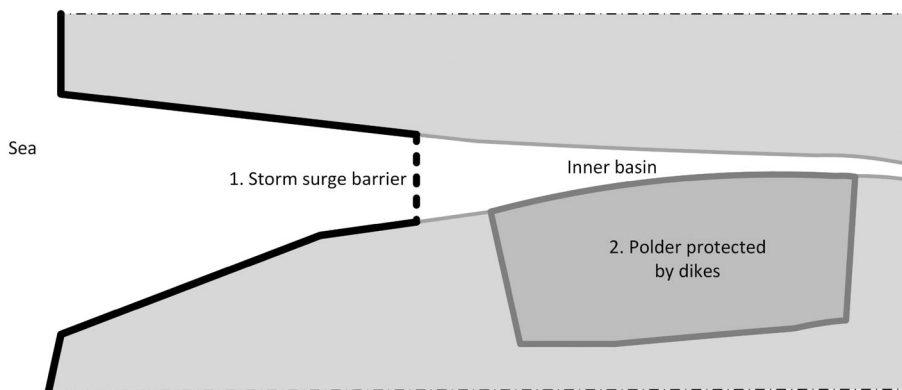
$$F_f = F_D \cdot P_{NC}. \tag{2}$$

In which F_D is the failure frequency of a dike (per year) and P_{NC} is the probability of a failed closure (on demand). In this paper, we consistently use frequency, with the corresponding symbol F, to describe the likeliness of an event to occur for a specified unit of time, in our case a year. For the likeliness of other events such as that of a failure to close, we apply the term probability with the corresponding symbol P.

The risk of a failed closure is often assumed to be independent from the risk of dike failure (see for instance HKV, 2006; Vader et al., 2022). The latter risk mainly

depends on the extreme water level maximum, that is, the highest water level during a storm, while closure reliability does not. Unavailability of electro-mechanical equipment often occurs in rest, due to dormant failures or equipment being under repair. Other unavailability of electro-mechanical equipment is related to the hydraulic conditions at the closure, which are not necessarily related to those at the peak of the storm. Software reliability is related to the complexity of the software, the production process, quality of software engineers and quality of testing (Van Manen et al., 2015). Reliability of human operation depends on staff and training quality

4 of 19 | WILEY—**CIWEM** Chartered Institution of Water and Environmental Management Journal of Flood Risk Management

MOOYAART ET AL.

(Lewin et al., 2003). None of these main reasons for a failure to close is, however, related to the water level maximum. Only a failed closure decision due to a too low water level forecast depends on the extreme water level maximum (Janssen & Jorissen, 1992). Often the closure criteria are chosen in a way, that this risk is insignificant. Therefore, we neglect the effect of the water level forecast error in this paper.

The failure probability of dikes highly depends on the water level maximum. For many failure modes such as inner slope erosion due to overflow & overtopping, geotechnical stability and groundwater erosion, the water level maximum is the most important load. Other loads such as wind waves are often related to the water level as well, as basins behind the barrier are often shallow. A modern approach is to consider the uncertainties in strength, load and models using fragility curves. The failure frequency of dikes is then a result of the frequency of extreme water levels and the probability of the dike failing given that extreme water level (Lendering et al., 2018).

As we are mainly interested in the basic choice between storm surge barrier and dike investments, we adopt a simplified approach. We assume dikes to resist the water level until a certain critical height H_D (metre r.t. mean sea-level [MSL]) (see Figure 3). Beyond this critical height, the dike will breach. Although this approach might seem highly simplified compared to the approach of Lendering et al. (2018), the optimization is not expected to be affected too much as in each approach the water level remains the most important factor. Both in older (van Dantzig, 1956) as more recent economic optimization models (Eijgenraam et al., 2014; Jonkman et al., 2009; Kind, 2014) the simplified approach was adopted to find optimal flood frequencies.

For the extreme water level distribution, we use an exponential distribution as initially proposed by Wemelsfelder (1939) and applied by van Dantzig (1956).

Although for extreme water level prediction, other extreme value distribution types such as the Generalised Extreme Value distribution are more common (Arns et al., 2013), the exponential distribution type has remained popular for economic optimization (Dupuits et al., 2017; Eijgenraam et al., 2017; Jonkman et al., 2009; Lendering et al., 2015). Furthermore, we assume the water level in front of the dike h_2 to be equal to the sea water level h_1, if the barrier is not closed. Hence, the exceedance probability of critical water levels H_D (metre r.t. MSL) is

$$F_D = F(h_1 > H_D) = 10^{-\frac{H_D - H_A}{H_B}}. \tag{3}$$

In which h_1 is the sea water level (metre r.t. MSL), H_A (metre r.t. MSL) is the water level which is exceeded annually on average. The distribution parameter H_B is the decimal height (m). With an increase of one decimal height, the extreme water level is 10 times less likely to occur. Combining Equations (2) and (3) results in the following equation for flood frequency:

$$F_f = 10^{-\frac{H_D - H_A}{H_B}} \cdot P_{NC}. \tag{4}$$

2.3 | Flood risk

Flood risk can be simplified to the product of flood frequency and its adverse economic consequences, when two assumptions are made (Lendering et al., 2020). First, the critical height approach has to be adopted, as was described in the previous section. Second, any dike breach is assumed to lead to maximum flood damage. At deep polders, a dike breach fills the polder with flood depths of several metres. With flood depths of 1–2 m, flood damages tend to be close to maximum damage. Wing et al. (2020) show this flood damage behaviour for
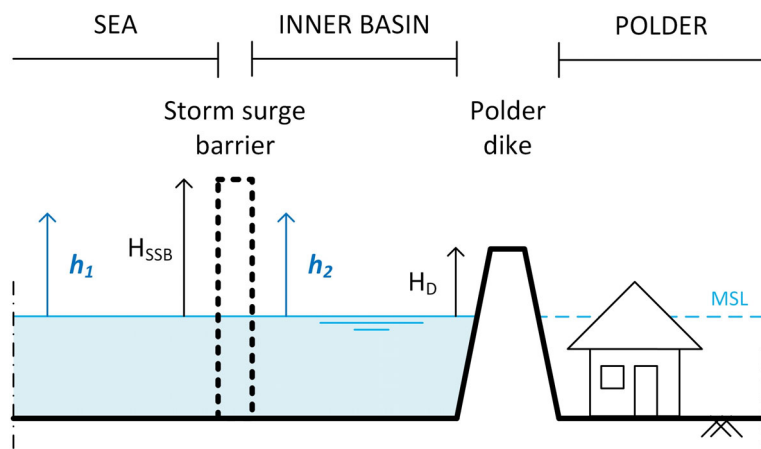

FIGURE 3 Schematic cross-section of a storm surge barrier flood protection system with one polder considered for the economic optimization model.

the deep polders of New Orleans. Therefore, at a deep polder, the loss D (M€) can be related to the sea water level h_1 (metre r.t. MSL) in the following manner:

$$D = \begin{cases} 0 & \text{if } h_1 < H_D \\ \hat{D} & \text{if } h_1 \geq H_D \end{cases}. \qquad (5)$$

Here, $\hat{D}$ is the maximum flood damage (M€).

To compare cost of flood risk reduction measures with residual flood risk, the present value of residual flood risk (R) needs to be determined. This value depends on inflation, interest, sea level rise, and the economic development in the protected area. Van Dantzig (1956) showed how the reduced discount rate δ' could be applied to account for all these effects. This approach, however, only accounts for sea level rising at a constant rate. As almost all current sea level projections show an accelerated pace, we calculate the reduced discount rate annually:

$$\delta' = \delta - \gamma - \beta. \qquad (6)$$

In which δ is the interest rate (per year), γ is the rate of economic growth and consequent damage increase (per year), and β is the rate at which flood risk increases due to (relative) sea level rise (per year). This latter rate β is equal to

$$\beta = \frac{r_{SLR}}{H_B} \cdot \ln 10, \qquad (7)$$

with r_{SLR} being the amount of sea level rise (m/year).

A period of 100 years is applied, as flood risk reduction measures often have a long lifetime. With this approach, the present value of the residual flood risk R (M€) is

$$R = F_f \cdot \hat{D} \cdot \sum_{0}^{100} (1 + \delta')^{-t}, \qquad (8)$$

with t being the number of years after the construction year of the flood protection measure (year).

2.4 | Cost functions

For the cost functions, the present value of the flood risk reduction measures is required. Therefore, the cost functions include construction, maintenance and operation cost. Although future sustainability is an important part of investment considerations, the present value of the

replacement after 100 years is small and, therefore, neglected in this paper.

Like van Dantzig (1956) and Jonkman et al. (2009), we take a cost relation for dike raise which consists of fixed cost and linearly rising cost with dike raise:

$$C_D = C_{D,0} + k_D \cdot (H_D - H_{D,0}). \qquad (9)$$

Here, C_D is the dike raise cost (M€), $C_{D,0}$ (M€) is the fixed investment cost, k_D is the additional cost per meter dike raise (M€ per m), $H_{D,0}$ is the initial critical dike level (metre r.t. MSL) and H_D is the raised critical dike level (metre r.t. MSL). Van Dantzig (1956) stressed that the linear approximation is only valid for small dike raises. Eijgenraam et al. (2014), therefore, proposed to apply an exponential cost relation. Kind (2014), however, demonstrates that the results of Eijgenraam et al. (2014) can be linearised. Moreover, empirical studies of the cost of dike raises could only find a linear relation (Aerts, 2018; Jonkman et al., 2013; Lenk et al., 2017), most likely due to the relatively large variation in cost. A linear cost function for dike raise, therefore, seems reasonable. Similarly, maintenance cost of dike raise is not well known. Therefore, we assume that the dike raise cost include maintenance and, therefore, is a present value.

For the case, we use both the construction and the maintenance and operation cost of the Maeslant barrier. The cost of improving closure reliability is not well known. For this paper, we assume that there are a discrete number of closure reliability improvements.

2.5 | Optimization of total cost

In this section, we explain how we find the solution with the least total cost, that is, the optimal solution. To optimise more effectively, we introduce three steps to narrow the selection of solutions. Only for the selected solutions, we determine the total costs. The objective of this approach is to only investigate amount of dike raises which can be optimal.

In the first step, we optimise dike raise without considering any closure reliability improvement, applying the model of Van Dantzig:

$$\Delta \check{H}_D = H_A - H_{D,0} - H_B \cdot \log\left(\frac{k_D \cdot H_B}{\ln(10) \cdot \hat{D} \cdot \sum (1+r)^t}\right). \qquad (10)$$

From this equation, it can be recognised that the optimal amount of dike raise is the sum of the yearly exceeded water level H_A, the initial dike height $H_{D,0}$ and
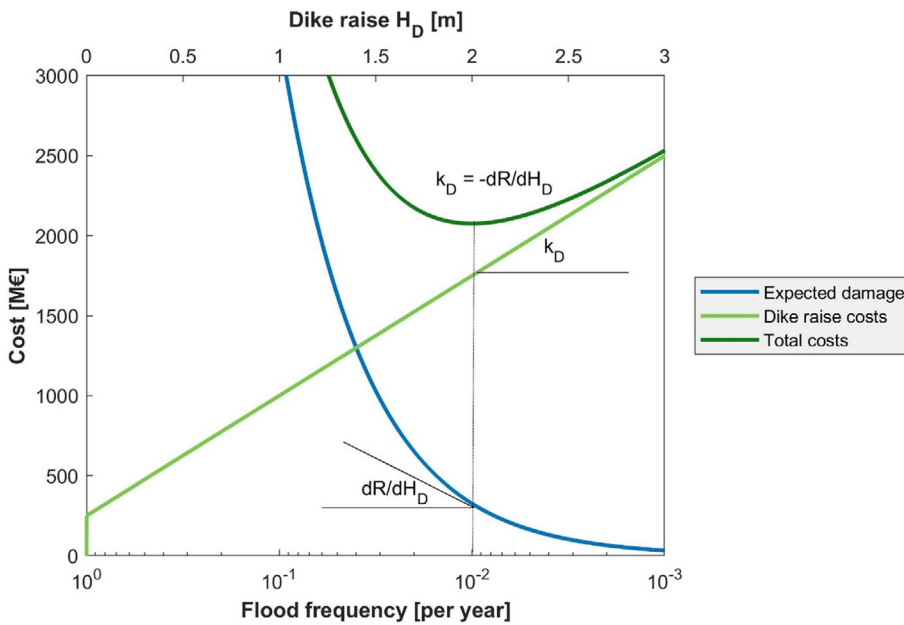
FIGURE 4 Classic optimization of dike raise with parameters: fixed costs dike raise $C_{D,0} = 250$ M€, variable cost dike raise $k_D = 750$ M€, initial dike height $H_{D,0}$ equal to yearly exceeded water level H_A, decimal height $H_B = 1.0$ m, maximal flood damage $\hat{D} = 650$ M€, reduced discount rate $\delta' = 2\%$. The optimal solution is a dike raise of 2 m, corresponding to a flood frequency of 1/100 years. At this optimum, the increase in dike raise cost (k_D) is opposite to the decline in risk (dR/dH_D).

a certain amount of decimal heights to optimally balance dike raise cost and risk. The term

$$\check{F}_{f,D} = \frac{k_D \cdot H_B}{\ln(10) \cdot \hat{D} \cdot \sum (1+r)^t} \quad (11)$$

corresponds to the optimal flood frequency with dike raise $\check{F}_{f,D}$ (per year). Figure 4 shows the principle of Van Dantzigs optimization method. At the optimal amount of dike raise (and flood frequency), the dike raise cost increases with the same rate that coastal flood risk declines (see Figure 4).

In the second step, we optimise the amount of dike raise for every closure reliability improvement, using a similar approach. With the use of Equations (2) and (11), the optimal failure frequency of the dike is established, including the probability of a failed closure:

$$\check{F}_D = \frac{k_D \cdot H_B}{P_{NC} \cdot \ln(10) \cdot \hat{D} \cdot \sum (1+r)^t}. \quad (12)$$

The optimal amount of dike raise is then

$$\Delta \check{H}_D = H_A - H_{D,0} - H_B \cdot \log(\check{F}_D). \quad (13)$$

To re-evaluate the equations, we consider a storm surge barrier with a probability of a failed closure of 1/100. Equation (12) shows that the optimal dike frequency is a factor 100 higher. This higher optimal dike frequency results in an optimal amount of dike raise which is two decimal heights lower.

Figure 5 shows another example to explain how to optimise combinations of closure reliability improvements and dike raise. Figure 5 is based on Figure 4, but has a closure reliability improvement, which costs 1000 M€ and has a probability of a failed closure of 4/100 per request. This improvement is illustrated with a grey arrow. The risk without any dike raise is 1300 M€, resulting in a total cost of 2300 M€, indicated with a black square. The light green line shows the additional cost for dike raise, which are the same as in Figure 4. As the risk curve and the dike raise costs are equal to the previous figure, also the optimum flood frequency is (10^{-2} per year). Hence, the optimal solution is to additionally raise the dike by 0.6 m. This combination of improvements leads to a total cost of 2000 M€, which is lower than (1) closure reliability alone and (2) dike raise alone.

Closure reliability improvements can lower flood frequency beyond the optimal flood frequency of dikes. In those cases, additional dike raise is never optimal anymore. Likewise, if closure reliability improvements lower flood frequency close to the optimal flood frequency of dikes, additional dike raise is infeasible. These additional dike raises are small, resulting in the cost being higher than the risk reduced. To overcome this issue, a selection criterion is introduced: the minimal amount of dike raise. At the minimal amount of dike raise, cost is exactly equal to the risk reduction dike raise achieves. This minimal amount of dike raise $\Delta H_{\min}$ (m) is (see Appendix A for the derivation)

FIGURE 5 Optimization with storm surge barrier improvement. Dike raise parameters are the same as the previous figure. Storm barrier improvement with a cost of 1000 M€ has a probability of a failed closure of 4/100 requests. The optimal solution is to combine this improvement with a dike raise of 0.6 m, resulting in a flood frequency of 1/100 years.
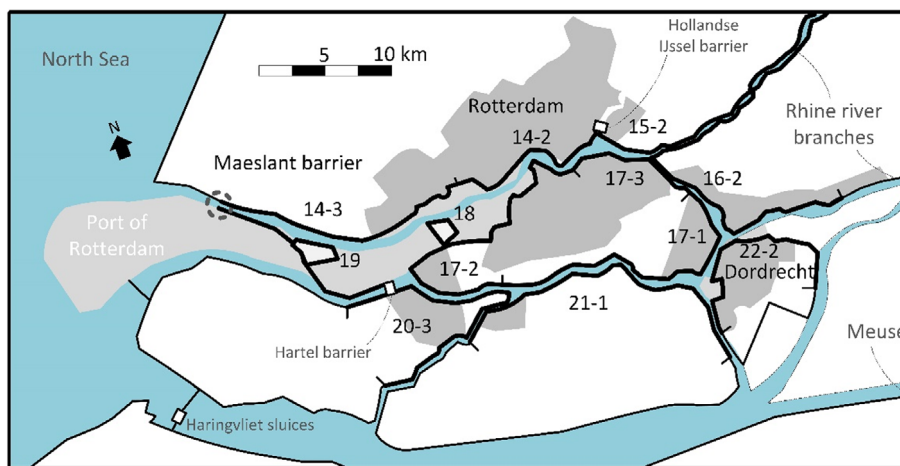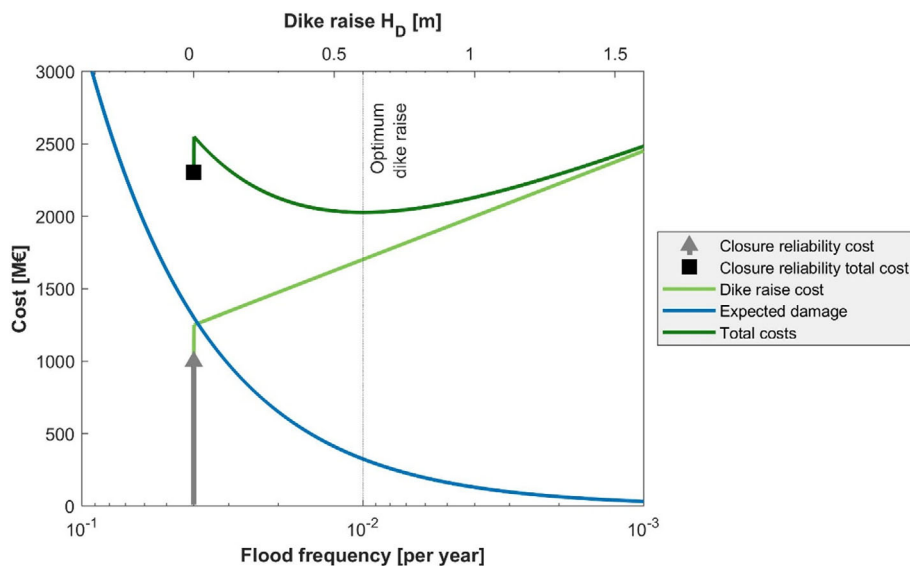
FIGURE 6 Map of dike ring parts (indicated with thick solid lines) significantly affected by the risk of a coastal flood due to a failed closure of the Maeslant barrier. Dike ring part numbers correspond to those presented by the Ministry of Infrastructure and Environment (2016). Thinner solid lines indicate dike rings which are not significantly affected by the Maeslant barrier. Thin dotted lines indicate river contours. Blue surfaces represent water bodies. Dark grey surfaces highlight inhabited areas behind dikes, while light grey indicates developed areas which are not protected by river dikes. Important hydraulic flood defence structures are represented by a square box.

$$\Delta H_{\min} = H_B \cdot \left(\frac{\Delta H_{\min} \cdot \ln 10}{H_B} + \frac{C_{D,0} \cdot \ln 10}{k_D \cdot H_B} + 1 \right). \quad (14)$$

In the final step, the optimal solution of the selected solutions is found using Equation (1).

3 | MAESLANT BARRIER CASE

3.1 | Area and potential flood damages

The Rhine and the Meuse flow in the North Sea at the south-western part of the Netherlands (see Figure 6). After the catastrophic 1953 flood, many of the river branches were closed off by dams. Because of the importance of the local port (Rotterdam), this waterway remained open. To balance flood risk and navigation interests, a storm surge barrier was constructed: The Maeslant barrier (construction year 1997). The model is illustrated on the basis of a case with this barrier.

The Maeslant barrier has most effect on floods directly behind the barrier. About 65 km upstream, flood risk depends only on river discharges. In nearby river branches, other hydraulic structures the Haringvliet sluices and the Hollandsche IJssel barrier also affect flood risk. Therefore, with a more reliable Maeslant barrier, flood risks following from river discharge or malfunctioning hydraulic structures become relatively more

important. Hence, improving reliability of the Maeslant barrier reduces the size of the area influencing coastal flood risk and vice versa. For this case though, we ignore this dependency and, therefore, take the size of the area influenced by Maeslant barrier to be constant. We use the area which is influenced with the current closure reliability of the Maeslant barrier, based on the study of HKV (2006).

A nationwide study was performed to estimate flood damages from dike breaches. Jongejan et al. (2013) describe the method applied to estimate flood damages. The results were reported per dike ring part, that is, a part of a dike ring where breaches result in approximately the same amount of damage (Ministry of Infrastructure and Environment, 2016). Table 1 provides expected flood damages for the dike ring parts affected by the Maeslant barrier.

The following parameters are applied for the extreme water level distribution: a yearly exceeded water level H_A of 2.1 m and a decimal height H_B of 0.75 m. Van Dantzig also applied these values. For frequencies between 1/100 and 1/100,000 years, the distribution corresponds well to the Generalised Pareto Distribution, which Deltares (2013) currently proposes to apply in flood risk assessments.

3.2 | Reduced discount rate

The reduced discount rate consists of four elements: interest, inflation, economic growth, and sea level rise. For the development of flood safety standards in the Netherlands, a combined rate for interest and inflation of 5.5% and an economic growth of 2% were applied (Kind, 2014), which are applied to this case as well. For sea level rise, we use the SSP2-4.5 scenario of the KNMI (2021), which is the middle of the three sea level projections presented. We applied linear regression to describe the rate of sea level rise:

$$r_{SLR} = 4.4 \cdot 10^{-5} \cdot (t + t_r) + 4.6 \cdot 10^{-3}, \quad (15)$$

in which t is the year number and t_r is a correction for the year of investment relative to the year of the sea level projection. As the sea level projection starts in 2005, while the price level of flood damages originates from 2011, a correction of 6 years is applied ($t_r = 6$).

3.3 | Storm surge barrier

The Maeslant barrier probability estimate of a failed closure is based on an extensive risk analysis using fault trees. A fault tree is a graphical model with logic gates that displays the various combinations of equipment failures, dependent failures, and human failures. Boolean algebra is used to quantify the probability of the top event (Henley & Kumamoto, 1981). The probability of a failed closure of the Maeslant barrier is approximately 1/100 per request.

Currently, no cost function is available for improvements of this probability of a failed closure. Therefore, we propose a cost function, using the existing Maeslant barrier as a reference. With respect to this reference, we take one major down- and upgrade: a barrier without redundant systems and a redundant barrier, respectively.

TABLE 1 Flood damages and costs to raise dikes at dike ring parts significantly affected by closure reliability of the Maeslant barrier.

Dike ring part name	Code	Flood damage (2011) (M€)	Costs to raise safety level with factor 10 (M€)
Zuid-Holland	14–2	12,000	132
	14–3	1700	89
Krimpenerwaard	15–2	19,000	180
Alblasserwaard	16–2	12,000	371
IJsselmonde	17–1	780	119
	17–2	2600	153
	17–3	11,000	24
Pernis	18–1	240	10
Rozenburg	19–1	1100	91
Voorne-Putten	20–3	5300	89
Hoekse Waard	21–1	1000	100
Eiland van Dordrecht	22–2	5300	226
Total		72,020	1584

We use a simplified fault tree of the Maeslant barrier to estimate the probabilities of failed closures of the three arrangements. Figure 7 shows the fault tree for this storm surge barrier. We assume all base systems to have the same failure probability: 1/100 per request. All backup systems are two times more likely to fail (1/50 per request). With this fault tree, probabilities of failed closures can be calculated in a simple manner with the use of two assumptions. First, the basic events are assumed to be independent. With an AND-gate, failure probabilities of basic events can then be multiplied to find the failure probability. Second, with OR-gates, as failure probabilities of the basic events are sufficiently small, the probability can be summed to estimate the failure probability. As a result, a single barrier with redundant systems has a probability of a failed closure of 1/100 per request, similar to the existing Maeslant barrier. The barrier without redundancies has a probability of a failed closure of 1/25 requests. The double barrier is about 10 times as reliable as the single barrier (see Appendix B).

For the cost of these three arrangements, we used actual construction cost and annual maintenance cost. The construction cost was retrieved from Mooyaart and Jonkman (2017) and corrected for the price level of 2011 (640 M€). Aerts et al. (2013) provided the maintenance

cost: 15 M€/year. Both the construction as the maintenance cost of the improvements of the power supply, control, and decision system is set at 10% of these costs, as generally, the costs of these systems are smaller than the cost of the storm surge barrier gate. A redundant barrier is assumed to have the same construction and maintenance cost as the initial barrier.

Table 2 shows the failure probabilities of the storm surge barrier systems and their redundancies. Table 3 presents the results of the fault tree analysis for the three storm surge barrier arrangements.

3.4 | Dike raise

Dikes along the inner basin of the Maeslant barrier vary in height and strength. Some dikes were already raised to resist sea water levels without a storm surge barrier and are, therefore, over-dimensioned up to about 2 m. On the other hand, many dikes such as those in the city centre of Rotterdam and Dordrecht proved difficult to raise, motivating the construction of a storm surge barrier. The existing dike in the city centre of Rotterdam is expected to breach with water levels higher than MSL + 3.6 m (Janssen & Jorissen, 1992). On average, this water level is expected to be exceeded once every 100 years without a
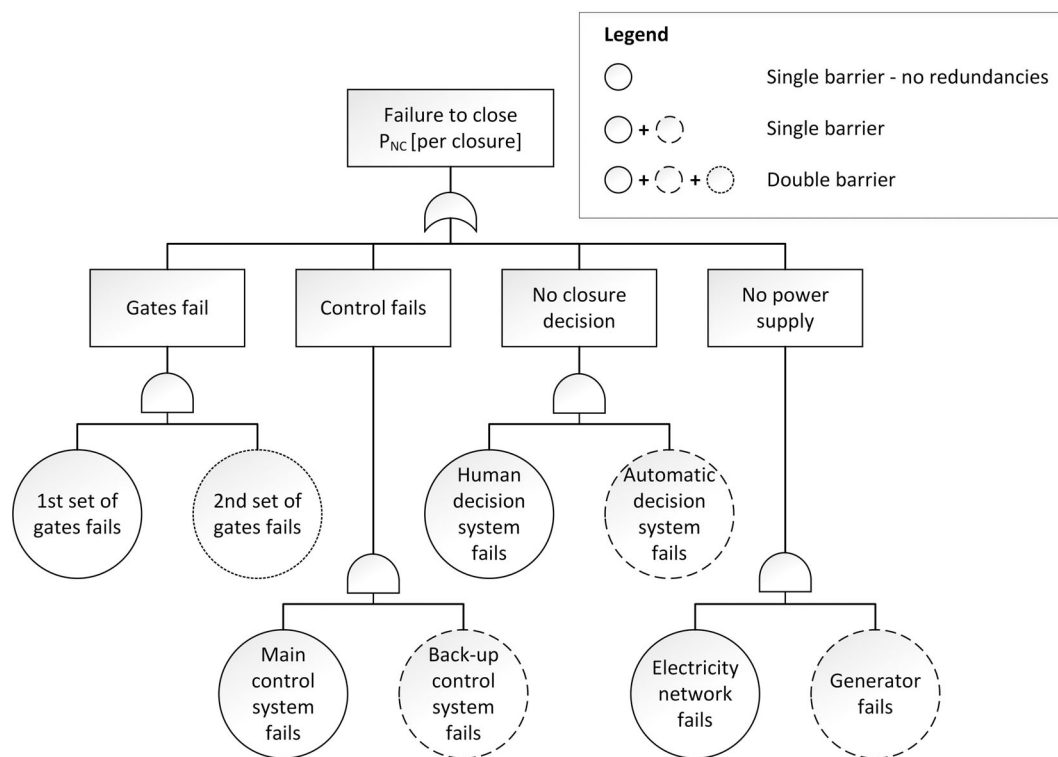
FIGURE 7 Simplified fault tree proposed for Maeslant barrier case. Basic events belonging to all storm surge barrier arrangements are indicated with solid borders. Basic events corresponding to a single and double barrier have dashed borders. The double barrier has an added basic event with a dotted border.

TABLE 2 Probabilities of basic events leading to failure of subsystems (on demand) of simplified fault tree for Maeslant barrier.

Item	Main system	Backup system	Combined
Gate	1×10^{-2}	2×10^{-2}	2×10^{-4}
Power supply	1×10^{-2}	2×10^{-2}	2×10^{-4}
Control	1×10^{-2}	2×10^{-2}	2×10^{-4}
Decision	1×10^{-2}	2×10^{-2}	2×10^{-4}

TABLE 3 Maeslant barrier closure reliability improvement cost relation.

#	Storm surge barrier arrangement	Cost (M€)	Probability of a failed closure P_{NC} (per request)
0	No barrier	0	1
1	Single barrier—no redundancies	810	4.0×10^{-2}
2	Single barrier	900	1.1×10^{-2}
3	Double barrier	1800	8.0×10^{-4}

storm surge barrier, corresponding with the exponential distribution proposed. For this case, we use this level as the initial critical water level of all dike ring parts considered. Furthermore, we assume all dike ring parts to fail if the critical water level is exceeded. Moreover, we only explore dike raise of all the dike ring parts combined.

For the study on flood safety standards, linear dike raise costs were reported (The Ministry of Infrastructure and Environment, 2016). The dike raise cost mentioned is the cost to lower the probability of dike failure with a factor 10 (corresponding to the product of dike raise cost per metre and decimal height: $k_D \times H_B$). Table 1 presents the cost per dike ring part.

No fixed cost is applied in this case. The Ministry of Infrastructure and Environment (2016) does not report any fixed cost. Moreover, Lenk et al. (2017) did not find any data to support fixed dike raise cost. Current dike raise optimization models often use other approaches to avoid small yearly raises. Brekelmans et al. (2012) assumed that dike raises are designed for a period of at least 40 years. In the results they present, the minimal dike raise is 25 cm. Van Dantzig (1956) used a minimal dike raise of 1 m. In the result section, we reflect on the relevance of estimating fixed cost.

4 | RESULTS

Before addressing the improvements, we reflect on the risk without any measure. Appendix C presents the present value calculation of flood damages, showing that the present value of all 100 years $(\hat{D}\sum(1+d')^t)$ amounts to 4.2×10^6 M€. Without any measure, the expected damage is 4.2×10^4 M€ (see Figure 8). This is a factor 100 lower as the dike breaches every 100 years on average.

Then, we use the optimization method to select solutions. First, we find the optimal amount of dike raise without storm surge barrier closure reliability improvements. This is 1.4 m (Equation 10), corresponding to a flood frequency of 1/6000 per year (Equation 11). Second, with Equations (12) and (13), the amounts of dike raises with closure reliability improvements are determined: 0.3, −0.1 and −1.0 m. The minimal dike raise is 0 m, as there is no fixed cost (see Equation 14). Only the single barrier without redundancies has a (positive) dike raise. Hence, for the final step, we selected six solutions: no measure, three closure reliability improvements, a dike raise of 1.4 m and a storm surge barrier without redundancies together with a dike raise of 0.3 m.

Figure 8 presents the total cost of the optimal possible solutions. Of the six remaining solutions, the single barrier has the lowest total cost (1300 M€), followed by the double barrier (1700 M€). Dike raise is almost three times as expensive as a single barrier (3500 M€). The single barrier without redundancies has a total cost of 2450 M€. Including dike raise with this closure reliability improvement, lowers the total cost with 300 M€.

4.1 | Sensitivity sea level rise

In this section, we explore the sensitivity of the results with respect to sea level rise. We assume that with an average rise in sea level, extreme water levels rise at the same pace. Hence, a 0.4 m average sea level rise raises the 1/100 year exceeded water level from MSL + 3.6 m to MSL + 4.0 m. Using this approach, the distribution parameter H_A of the exponential distribution changes with sea level rise SLR. For sea level rises until 1.0 m, optimal solutions were derived.

FIGURE 8 Total costs for selected solutions of Maeslant barrier case. The blue, grey, and green costs correspond with the risk, storm surge barrier costs, and dike raise costs, respectively. With a dashed line, the minimum total costs are indicated. The selected solutions are: (0) no measure, (1) single barrier without redundancies, (2) single barrier with redundancies, (3) double barrier, (D) 1.4 m dike raise and (D + 1) 0.3 m dike raise with a single barrier without redundancies.
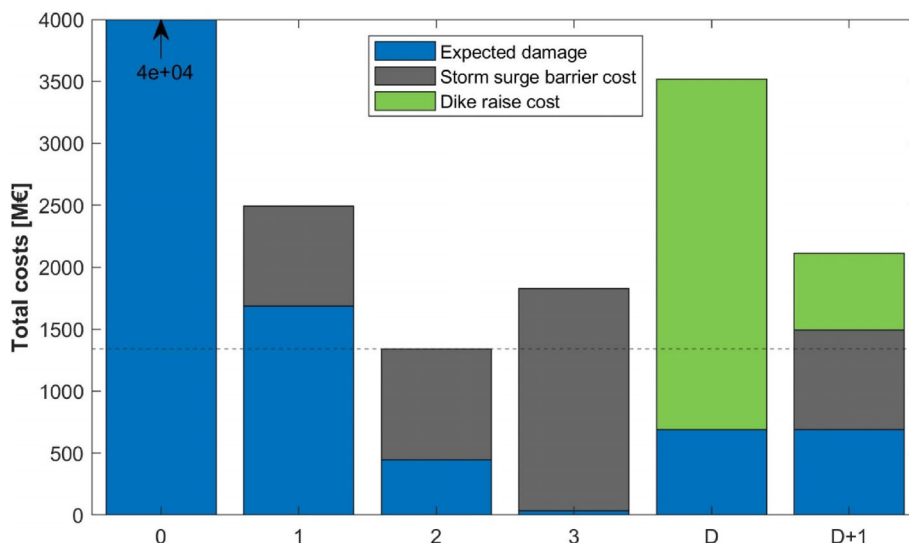
FIGURE 9 Total costs of optimal solutions with increasing sea level rise. The grey, green, and blue hatched areas indicate the storm surge barrier improvement costs, dike raise, and expected flood damage, respectively. The costs of the three storm surge barrier improvements are indicated with a dotted line. At the horizontal axis, the year corresponding to the amount of sea level rise according to scenario SSP2-4.5 (50%) is mentioned.
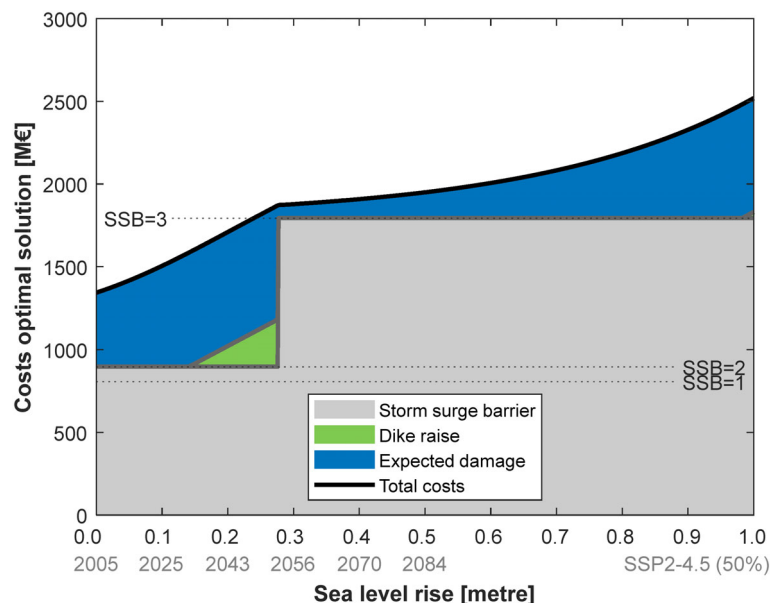
Figure 9 presents the total cost of the optimal solution. Until a sea level rise of approximately 0.15 m, a single barrier without dike raise is optimal. Beyond approximately 0.25 m, a double barrier is the solution with the least total cost. Between these sea level rises, a single barrier including a small amount of dike raise (0–0.2 m) is found to be optimal. This latter result is surprising, as normally these small amounts of dike raise are uneconomical. The model produces this result for two reasons: (1) no fixed cost or minimal life time of dike raise are assumed and (2) there are no closure reliability improvements in between a single and double barrier.

Figure 10 presents the flood frequency of the optimal solution. If only storm surge barrier improvements are optimal, the optimal flood frequency varies, due to the discrete nature of the improvements. When storm surge barrier improvements are combined with dike raise, the

optimal flood frequency is constant and equal to the optimal flood frequency of dikes. Because there are no fixed dike raise cost in this case, optimal solutions with storm surge barrier improvements always have a lower flood frequency than the dike raise optimal flood frequency.

From the results, we can deduct an optimal strategy with respect to sea level rise. Until a sea level rise of 0.15 m, the current situation is economically optimal. Beyond this sea level rise, small dike raises or a double barrier can be considered.

5 | DISCUSSION

This section discusses the case study's results and the models broader applicability. The case study motivates the construction of the Maeslant barrier. Although with
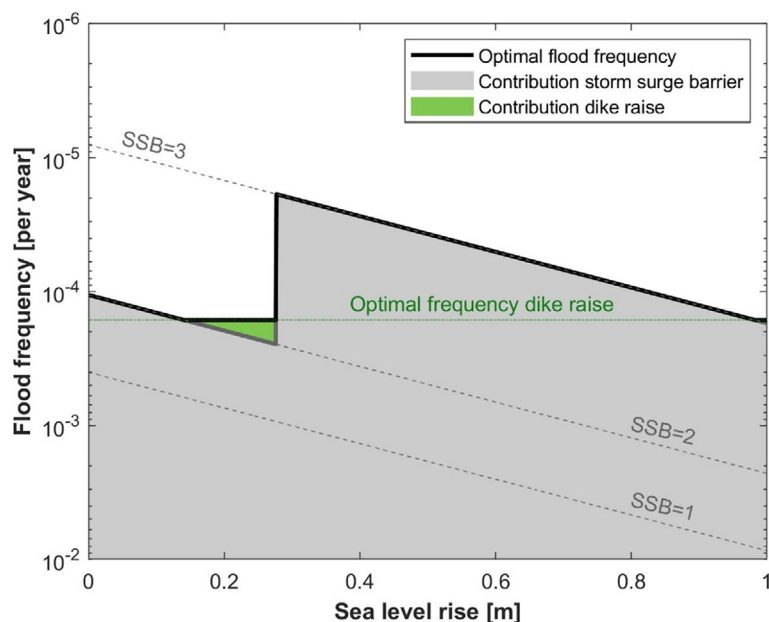
FIGURE 10 Optimal flood frequencies with increasing sea level rise. The grey and green hatched areas indicate which part of the optimal flood frequency can be contributed to storm surge barrier improvements and dike raise, respectively. A green dashed line indicates the optimal flood probability with dike raise alone. The flood frequency for the three investigated storm surge barrier improvements is indicated with a dotted line. These flood frequencies increase, because the initial dike height stays constant while extreme water levels become more frequent with sea level rise.

respect to the dikes behind the barrier, some highly simplified approaches were taken such as a ignoring spatial variability of dike heights and ignoring the fragility of dikes, we do not expect these assumptions to greatly affect the result. Furthermore, only areas protected by dikes were considered. If those areas in front of the dikes but behind the barrier were included, storm surge barrier closure reliability improvements would become even more favourable. Hence, substantial investments such as a double barrier might become feasible with a sea level rise even smaller than the 0.15–0.25 m which the sensitivity analysis indicated. Although not included in the cost function, substantial investments in between a single and double barrier with an intermediate effect on flood risk seem most promising. Examples of such improvements are: more reliable equipment, optimised test procedures, or (even) better trained staff. Based on the results of this study, a better understanding of the costs and benefit of these types of improvements is most important to come to an economic optimal solution.

In addition, most parameters in the model have considerable uncertainty. Probably most important are climate change effects and discount rates. In this case, only mild projections with respect to sea level rises were considered. If more extreme sea level rise projections are considered, larger investments become economic. On the other hand, there are also uncertainties with respect to interest rate and economic growth, which might motivate to await larger investments. To account for these and other uncertainties, the robustness of the measures needs to be tested.

Although for the Maeslant barrier the model seems applicable for short-term economic decision making due

to the current dominance of the failure to close risk, other risks and effects are to be considered for long-term decision making and a wider applicability of the model. A risk framework is required which considers possibilities of structural, non-opening, a water level forecast error, overtopping and overflowing, but also flood risks with successful barrier closures. Moreover, more effective flood risk measures can hinder navigation and tidal exchange. In order to consider these types of flood risk measures, more insight is required into the economic value of navigation and tidal exchange hindrance during storm surges.

6 | CONCLUDING REMARKS

This research aimed to develop a method to effectively optimise coastal flood defence systems with a storm surge barrier. Closure reliability was identified as an important parameter for economic optimization. A model was developed to show how closure reliability affects economic decision-making, balancing coastal flood risk with investments in closure reliability and dike raise.

The model was applied at the region protected by the Maeslant barrier. The model results substantiated the decision to construct the Maeslant barrier. Moreover, we demonstrated that large investments such as a redundant barrier are already economically sound with a few decimetres of sea level rise.

Based on our experience with this case, we expect that the proposed model can support many studies. Storm surge barrier managers can apply the model to support large maintenance investments. Regional flood

authorities can balance storm surge barrier improvements with local measures to protect the area behind the barrier. The model can be used at feasibility studies of new storm surge barriers such as New York, Goteborg, Galveston, and Shanghai. Finally, the model can assist in finding appropriate strategies to compensate for sea level rise and other effects raising coastal flood risk.

DATA AVAILABILITY STATEMENT
Data sharing not applicable to this article as no datasets were generated or analysed during the current study.

ORCID
Leslie F. Mooyaart https://orcid.org/0000-0003-2571-4045

REFERENCES
Aerts, J. C. J. H., Botzen, W. J. W., de Moel, H., & Bowman, M. (2013). Cost estimates for flood resilience and protection strategies in New York City. *Annals of the New York Academy of Sciences*, *1294*(1), 1–104. https://doi.org/10.1111/nyas.12200

Aerts, J. C. (2018). A review of cost estimates for flood adaptation. *Water (Switzerland)*, *10*(11), 1646.

Aerts, J. C., Botzen, W. J., Emanuel, K., Lin, N., De Moel, H., & MichelKerjan, E. O. (2014). Climate adaptation: Evaluating flood resilience strategies for coastal megacities. *Science*, *344*(6183), 473–475.

Arns, A., Wahl, T., Haigh, I. D., Jensen, J., & Pattiaratchi, C. (2013). Estimating extreme water level probabilities: A comparison of the direct methods and recommendations for best practise. *Coastal Engineering*, *81*, 51–66.

Brekelmans, R., den Hertog, D., Roos, K., & Eijgenraam, C. (2012). Safe dike heights at minimal costs: The nonhomogeneous case. *Operations Research*, *60*(6), 1342–1355.

Calafat, F. M., Wahl, T., Tadesse, M. G., & Sparrow, S. N. (2022). Trends in Europe storm surge extremes match the rate of sea-level rise. *Nature*, *603*(7903), 841–845.

Ceres, R. L., Forest, C. E., & Keller, K. (2019). Optimization of multiple storm surge risk mitigation strategies for an Island City on a wedge. *Environmental Modelling and Software*, *119*, 341–353.

Ceres, R. L., Forest, C. E., & Keller, K. (2022). Trade-offs and synergies in managing coastal flood risk: A case study for New York City. *Journal of Flood Risk Management*, *15*(1), 1–12.

CPB Netherlands Bureau for Economic Policy Analysis. (2013). *Economic optimal safety at the IJssel Lake area (Dutch: Economisch optimale waterveiligheid in het IJsselmeergebied). Technical report*. CPB.

Deltares. (2013). *Representative values coastal waters and large rivers (Dutch: Kenmerkende waarden kustwateren en grote rivieren). Technical report*. Deltares.

Dupuits, E. J., Schweckendiek, T., & Kok, M. (2017). Economic optimization of coastal flood defense systems. *Reliability Engineering and System Safety*, *159*, 143–152.

Eijgenraam, C., Brekelmans, R., Den Hertog, D., & Roos, K. (2017). Optimal strategies for flood prevention. *Management Science*, *63*, 1644–1656.

Eijgenraam, C., Kind, J., Bak, C., Brekelmans, R., Den Hertog, D., Duits, M., Roos, K., Vermeer, P., & Kuijken, W. (2014). Economically efficient standards to protect the Netherlands against flooding. *Interfaces*, *44*, 7–21.

Groves, D. G., & Sharon, C. (2013). Planning tool to support planning the future of coastal Lousiana. *Journal of Coastal Research*, *67*, 147–161.

Haasnoot, M., Kwakkel, J. H., & Walker, W. E. (2013). Dynamic adaptive policy pathways: A method for crafting robust decisions for a deeply uncertain world. *Global Environmental Change*, *23*(2), 485–498.

Hallegatte, S., Green, C., Nicholls, R. J., & Corfee-Morlot, J. (2013). Future flood losses in major coastal cities. *Nature Climate Change*, *3*(9), 802–806.

Henley, E. J., & Kumamoto, H. (1981). *Reliability engineering and risk assessment*. Preston Hall.

HKV. (2006). *Achterlandstudie Maeslantkering, Hydra-B. Technical report*. HKV Lijn in Water. https://edepot.wur.nl/498344

Janssen, J. P., & Jorissen, R. E. (1992). Integrating forecast effects and operational behaviour in designing the Rotterdam storm surge barrier. In *Floods and flood management. Fluid mechanics and its applications*. Springer.

Jongejan, R., Maaskant, B., Horst, W. T., Havinga, F., Roode, N., & Stefess, H. (2013). The VNK2-project: A fully probabilistic risk analysis for all major levee systems in the Netherlands. *IAHS-AISH Publication*, *357*, 75–85.

Jonkman, S. N., Hillen, M. M., Nicholls, R. J., Kanning, W., & van Ledden, M. (2013). Costs of adapting coastal defences to sea-level rise—New estimates and their implications. *Journal of Coastal Research*, *290*, 1212–1226.

Jonkman, S. N., Kok, M., Van Ledden, M., & Vrijling, J. K. (2009). Riskbased design of flood defence systems: A preliminary analysis of the optimal protection level for the New Orleans metropolitan area. *Journal of Flood Risk Management*, *2*, 170–181.

Kim, M. J., Nicholls, R. J., Preston, J. M., & de Almeida, G. A. (2019). An assessment of the optimum timing of coastal flood adaptation given sealevel rise using real options analysis. *Journal of Flood Risk Management*, *12*, 1–28.

Kind, J. M. (2014). Economically efficient flood protection standards for the Netherlands. *Journal of Flood Risk Management*, *7*, 103–117.

KNMI. (2021). *Klimaatsignaal'21. Technical report*. KNMI. https://cdn.knmi.nl/knmi/asc/klimaatsignaal21/KNMI_Klimaatsignaal21.pdf

Lendering, K., Jonkman, S., van Ledden, M., & Vrijling, J. (2020). Defend or raise? Optimising flood risk reduction strategies. *Journal of Flood Risk Management*, *13*, e12553.

Lendering, K., Schweckendiek, T., & Kok, M. (2018). Quantifying the failure probability of a canal levee. *Georisk*, *9518*, 1–15.

Lendering, K. T., Jonkman, S. N., Van Gelder, P. H., & Peters, D. J. (2015). Risk-based optimization of land reclamation. *Reliability Engineering and System Safety*, *144*, 193–203.

Lenk, S., Rybski, D., Heidrich, O., Dawson, R. J., & Kropp, J. P. (2017). Costs of sea dikes-regressions and uncertainty estimates. *Natural Hazards and Earth System Sciences*, *17*(5), 765–779.

14 of 19 | WILEY—**CIWEM** Chartered Institution of Water and Environmental Management | Journal of **Flood Risk Management**

MOOYAART ET AL.

Lewin, J., Ballard, G., & Bowles, D. S. (2003). Spillway gate reliability in context of overall dam failure risk. In *USSD Annual Lecture* (pp. 1–17). Charleston.

Ministry of Infrastructure and Environment. (2016). *Factsheets flood safety standards primary flood defences (Dutch: Factsheets normering primaire waterkeringen). Technical report.* https://www.helpdeskwater.nl/publish/pages/132790/factsheets_compleet19122016.pdf

Mooyaart, L. F., & Jonkman, S. N. (2017). Overview and design considerations of storm surge barriers. *Journal of Waterway, Port, Coastal, and Ocean Engineering*, *143*(4), 06017001.

Rijkswaterstaat. (2002). *Project note/EIA Ramspol barrier, Hydraulic boundary conditions (Dutch: Projectnota/MER keersluis Ramspol, Hydraulische randvoorwaarden). Technical report.* Rijkswaterstaat. https://puc.overheid.nl/rijkswaterstaat/doc/PUC_50209_31/

Rijkswaterstaat. (2008). *Performance levels Eastern Scheldt, continuation (Dutch: Prestatiepeilen Oosterschelde, vervolg). Technical report.* Rijkswaterstaat. https://puc.overheid.nl/rijkswaterstaat/doc/PUC_50209_31/

Ruig, L. T. D., Barnard, P. L., Botzen, W. J. W., Grifman, P., Finzi, J., Moel, H. D., Sadrpour, N., & Aerts, J. C. J. H. (2019). An economic evaluation of adaptation pathways in coastal mega cities: An illustration for Los Angeles. *Science of the Total Environment*, *678*, 647–659.

Vader, H., Bakker, A. M., Jonkman, S. N., van den Boomen, M., van Baaren, E., & Diermanse, F. L. (2022). A framework for assessing the remaining life of storm surge barriers. (submitted for publication).

van Berchum, E. C., Mobley, W., Jonkman, S. N., Timmermans, J. S., Kwakkel, J. H., & Brody, S. D. (2019). Evaluation of flood risk reduction strategies through combinations of interventions. *Journal of Flood Risk Management*, *12*, 1–17.

van Berchum, E. C., van Ledden, M., Timmermans, J. S., Kwakkel, J. H., & Jonkman, S. N. (2020). Rapid flood risk screening model for compound flood events in Beira, Mozambique. *Natural Hazards and Earth System Sciences*, *20*(10), 2633–2646.

van Dantzig, D. (1956). Economic decision problems for flood protection. *Econometrica*, *24*(3), 276–287.

van der Pol, T., Hinkel, J., Merkens, J., MacPherson, L., Vafeidis, A. T., Arns, A., & Dangendorf, S. (2021). Regional economic analysis of flood defence heights at the German Baltic Sea coast: A multi-method cost-benefit approach for flood prevention. *Climate Risk Management*, *32*, 100289.

Van Manen, S., Brandt, E., Van Ekris, J., & Geurts, W. (2015). TOPAAS: An alternative approach to software reliability quantification. *Quality and Reliability Engineering International*, *31*(2), 183–191.

Vezér, M., Bakker, A., Keller, K., & Tuana, N. (2018). Epistemic and ethical trade-offs in decision analytical modelling: A case study of flood risk management in New Orleans. *Climatic Change*, *147*(1–2), 1–10.

Wemelsfelder, P. (1939). Wetmatigheden in het optreden van stormvloeden. *De Ingenieur*, *54*(9), 31–35.

Wing, O. E., Pinter, N., Bates, P. D., & Kousky, C. (2020). New insights into US flood vulnerability revealed from flood insurance big data. *Nature Communications*, *11*(1), 1–10.

APPENDIX A: DERIVATION OF MINIMAL DIKE RAISE

The minimal dike raise is the smallest amount of dike raise at which dike raise can possibly be optimal:

$$\Delta H_{\min} = \check{H}_D - H_{D,0}. \tag{A1}$$

In which $\check{H}_D$ (metre r.t. MSL) is the optimal dike level and $H_{D,0}$ (metre r.t. MSL) the initial dike height. At minimal dike raise $\Delta H_{\min}$, costs of dike raise are equal to the risk reduction that dike raise achieves, that is,

$$C = \Delta R. \tag{A2}$$

With the use of Equation (8) (Section 2.2) and Equation (9) (Section 2.3), this can be written as

$$C_{D,0} + k_D \cdot \Delta H_{\min} = \Delta F \cdot \hat{D} \cdot \sum_0^{100} (1 + d')^t. \tag{A3}$$

The flood frequency difference is as a result of the minimal dike raise is

$$\begin{aligned}\Delta F &= F(h_1 > H_{D,0}) - F(h_1 > \check{H}_D) = \dots \\ &10^{-\frac{\check{H}_D - \Delta H_{\min} - H_A}{H_B}} - 10^{-\frac{\check{H}_D - H_A}{H_B}} = \dots \\ &10^{-\frac{\check{H}_D - H_A}{H_B}} \cdot \left(10^{-\frac{\Delta H_{\min}}{H_B}} - 1\right).\end{aligned} \tag{A4}$$

The optimal flood frequency for dike raise is (see Equation 11, Section 2.4)

$$F(h_1 \geq \check{H}_D) = 10^{-\frac{\check{H}_D - H_A}{H_B}} = \frac{k_D \cdot H_B}{\ln(10) \cdot \hat{D} \cdot \sum_0^{100} (1 + d')^t}. \tag{A5}$$

With the use of Equations A4 and A5, Equation A3 becomes

$$C_{D,0} + k_D \cdot \Delta H_{\min} = \frac{k_D \cdot H_B}{\ln(10)} \cdot \left(10^{-\frac{\Delta H_{\min}}{H_B}} - 1\right). \tag{A6}$$

Then by rearranging, the following relation is found:

$$\Delta H_{\min} = H_B \cdot \log\left(\frac{\Delta H_{\min} \cdot \ln(10)}{H_B} + \frac{C_{D,0} \cdot \ln(10)}{k_D \cdot H_B} + 1\right). \tag{A7}$$

Using iteration, the minimal dike raise can be calculated.

APPENDIX B: CALCULATION STEPS AND- AND OR-GATES

Logic gates perform a logical operation based on one or more inputs resulting in one output. In this appendix, we show the calculation steps in the case of two (input) events A and B resulting in (output) event C. We only present two types of logic gates: the AND- and OR-gate.

With the AND-gate, both event A and B have to occur for event C to take place. The probabilities of these events are described by P_A, P_B, P_C, respectively. If events A and B are independent, the probability of event C is:

$$P_C = P_A \cdot P_B$$

With the OR-gate, either event A or B has to occur for event C to take place. If the events are independent and the probabilities of events A and B are small ($<1/10$), the probability of event C can be estimated by:

$$P_C = P_A + P_B$$

We apply these equations to find the probabilities of failed closures for three system arrangements:

i. Maeslant barrier with only main systems.
ii. Maeslant barrier with backup systems for the power supply, control and decision system.
iii. Maeslant barrier with all backup systems including a second gate.

The probabilities of failure events of main and backup systems are presented in Table B1. In bold, the indices are presented per system. For instance, the probability of failure of the main system of the gate is described by the symbol P_{G1} and its backup system by P_{G2}.

For the arrangement with only main systems (i), the probability of a failed closure is then:

$$P_{NC,i} = P_{G1} + P_{P1} + P_{C1} + P_{D1} = \dots$$

Item	Main system (1)	Backup system (2)	Combined
Gate (**G**)	1×10^{-2}	2×10^{-2}	2×10^{-4}
Power supply (**P**)	1×10^{-2}	2×10^{-2}	2×10^{-4}
Control (**C**)	1×10^{-2}	2×10^{-2}	2×10^{-4}
Decision (**D**)	1×10^{-2}	2×10^{-2}	2×10^{-4}

TABLE B1   Probabilities of basic events leading to failure of subsystems (on demand) of simplified fault tree for Maeslant barrier. In bold, the indices applied are presented.

$$...10^{-2} + 10^{-2} + 10^{-2} + 10^{-2} = \mathbf{4 \cdot 10^{-2}}.$$

For the arrangement with backup systems for the power supply, control and decision system (ii), the probability of a failed closure is:

$$P_{NC,ii} = P_{G1} + P_{P1} \cdot P_{P2} + P_{C1} \cdot P_{C2} + P_{D1} \cdot P_{D2} = ...$$

$$...10^{-2} + 10^{-2} \cdot 2 \cdot 10^{-2} + 10^{-2} \cdot 2 \cdot 10^{-2} + 10^{-2} \cdot 2 \cdot 10^{-2} = \mathbf{10^{-2}}$$

For the arrangement with all backup systems including a second gate (iii), the probability of a failed closure is:

$$P_{NC,iii} = P_{G1} \cdot P_{G2} + P_{P1} \cdot P_{P2} + P_{C1} \cdot P_{C2} + P_{D1} \cdot P_{D2} =$$

$$...10^{-2} \cdot 2 \cdot 10^{-2} + 10^{-2} \cdot 2 \cdot 10^{-2} + 10^{-2} \cdot 2 \cdot 10^{-2}$$
$$+ 10^{-2} \cdot 2 \cdot 10^{-2}$$
$$= \mathbf{8 \cdot 10^{-4}}$$

APPENDIX C: PRESENT VALUE CALCULATION

Year	Year number	Discount rate	Present cost storm surge barrier (M€)	Rate of sea level rise (m/year)	Reduced discount rate	Present value flood damage (M€)
2011	0	5.5%	6.40E+02	0.0049	2.0%	0.00E+00
2012	1	5.5%	1.42E+01	0.0049	2.0%	7.06E+04
2013	2	5.5%	1.34E+01	0.0050	2.0%	6.92E+04
2014	3	5.5%	1.27E+01	0.0050	2.0%	6.79E+04
2015	4	5.5%	1.20E+01	0.0050	2.0%	6.66E+04
2016	5	5.5%	1.13E+01	0.0051	1.9%	6.53E+04
2017	6	5.5%	1.07E+01	0.0051	1.9%	6.41E+04
2018	7	5.5%	1.01E+01	0.0052	1.9%	6.29E+04
2019	8	5.5%	9.54E+00	0.0052	1.9%	6.18E+04
2020	9	5.5%	9.02E+00	0.0053	1.9%	6.07E+04
2021	10	5.5%	8.52E+00	0.0053	1.9%	5.96E+04
2022	11	5.5%	8.05E+00	0.0053	1.9%	5.86E+04
2023	12	5.5%	7.61E+00	0.0054	1.8%	5.76E+04
2024	13	5.5%	7.19E+00	0.0054	1.8%	5.66E+04
2025	14	5.5%	6.79E+00	0.0055	1.8%	5.57E+04
2026	15	5.5%	6.42E+00	0.0055	1.8%	5.48E+04
2027	16	5.5%	6.07E+00	0.0056	1.8%	5.39E+04
2028	17	5.5%	5.73E+00	0.0056	1.8%	5.31E+04
2029	18	5.5%	5.42E+00	0.0057	1.8%	5.23E+04
2030	19	5.5%	5.12E+00	0.0057	1.8%	5.15E+04
2031	20	5.5%	4.84E+00	0.0057	1.7%	5.07E+04
2032	21	5.5%	4.57E+00	0.0058	1.7%	5.00E+04
2033	22	5.5%	4.32E+00	0.0058	1.7%	4.93E+04
2034	23	5.5%	4.08E+00	0.0059	1.7%	4.86E+04
2035	24	5.5%	3.86E+00	0.0059	1.7%	4.79E+04
2036	25	5.5%	3.65E+00	0.0060	1.7%	4.73E+04
2037	26	5.5%	3.45E+00	0.0060	1.7%	4.67E+04
2038	27	5.5%	3.26E+00	0.0061	1.6%	4.61E+04
2039	28	5.5%	3.08E+00	0.0061	1.6%	4.55E+04
2040	29	5.5%	2.91E+00	0.0061	1.6%	4.49E+04
2041	30	5.5%	2.75E+00	0.0062	1.6%	4.44E+04
2042	31	5.5%	2.60E+00	0.0062	1.6%	4.38E+04
2043	32	5.5%	2.45E+00	0.0063	1.6%	4.33E+04
2044	33	5.5%	2.32E+00	0.0063	1.6%	4.29E+04
2045	34	5.5%	2.19E+00	0.0064	1.5%	4.24E+04
2046	35	5.5%	2.07E+00	0.0064	1.5%	4.19E+04
2047	36	5.5%	1.96E+00	0.0064	1.5%	4.15E+04
2048	37	5.5%	1.85E+00	0.0065	1.5%	4.11E+04
2049	38	5.5%	1.75E+00	0.0065	1.5%	4.07E+04
2050	39	5.5%	1.65E+00	0.0066	1.5%	4.03E+04

18 of 19 | WILEY—**CIWEM** Chartered Institution of Water and Environmental Management Journal of Flood Risk Management

MOOYAART ET AL.

Year	Year number	Discount rate	Present cost storm surge barrier (M€)	Rate of sea level rise (m/year)	Reduced discount rate	Present value flood damage (M€)
2051	40	5.5%	1.56E+00	0.0066	1.5%	3.99E+04
2052	41	5.5%	1.48E+00	0.0067	1.5%	3.95E+04
2053	42	5.5%	1.39E+00	0.0067	1.4%	3.92E+04
2054	43	5.5%	1.32E+00	0.0068	1.4%	3.88E+04
2055	44	5.5%	1.24E+00	0.0068	1.4%	3.85E+04
2056	45	5.5%	1.18E+00	0.0068	1.4%	3.82E+04
2057	46	5.5%	1.11E+00	0.0069	1.4%	3.79E+04
2058	47	5.5%	1.05E+00	0.0069	1.4%	3.76E+04
2059	48	5.5%	9.93E−01	0.0070	1.4%	3.74E+04
2060	49	5.5%	9.38E−01	0.0070	1.3%	3.71E+04
2061	50	5.5%	8.87E−01	0.0071	1.3%	3.68E+04
2062	51	5.5%	8.38E−01	0.0071	1.3%	3.66E+04
2063	52	5.5%	7.92E−01	0.0072	1.3%	3.64E+04
2064	53	5.5%	7.48E−01	0.0072	1.3%	3.62E+04
2065	54	5.5%	7.07E−01	0.0072	1.3%	3.60E+04
2066	55	5.5%	6.68E−01	0.0073	1.3%	3.58E+04
2067	56	5.5%	6.31E−01	0.0073	1.3%	3.56E+04
2068	57	5.5%	5.97E−01	0.0074	1.2%	3.54E+04
2069	58	5.5%	5.64E−01	0.0074	1.2%	3.53E+04
2070	59	5.5%	5.33E−01	0.0075	1.2%	3.51E+04
2071	60	5.5%	5.04E−01	0.0075	1.2%	3.50E+04
2072	61	5.5%	4.76E−01	0.0075	1.2%	3.49E+04
2073	62	5.5%	4.50E−01	0.0076	1.2%	3.47E+04
2074	63	5.5%	4.25E−01	0.0076	1.2%	3.46E+04
2075	64	5.5%	4.02E−01	0.0077	1.1%	3.45E+04
2076	65	5.5%	3.79E−01	0.0077	1.1%	3.44E+04
2077	66	5.5%	3.59E−01	0.0078	1.1%	3.44E+04
2078	67	5.5%	3.39E−01	0.0078	1.1%	3.43E+04
2079	68	5.5%	3.20E−01	0.0079	1.1%	3.42E+04
2080	69	5.5%	3.03E−01	0.0079	1.1%	3.42E+04
2081	70	5.5%	2.86E−01	0.0079	1.1%	3.41E+04
2082	71	5.5%	2.70E−01	0.0080	1.0%	3.41E+04
2083	72	5.5%	2.55E−01	0.0080	1.0%	3.41E+04
2084	73	5.5%	2.41E−01	0.0081	1.0%	3.41E+04
2085	74	5.5%	2.28E−01	0.0081	1.0%	3.41E+04
2086	75	5.5%	2.16E−01	0.0082	1.0%	3.41E+04
2087	76	5.5%	2.04E−01	0.0082	1.0%	3.41E+04
2088	77	5.5%	1.92E−01	0.0083	1.0%	3.41E+04
2089	78	5.5%	1.82E−01	0.0083	1.0%	3.41E+04
2090	79	5.5%	1.72E−01	0.0083	0.9%	3.42E+04
2091	80	5.5%	1.62E−01	0.0084	0.9%	3.42E+04
2092	81	5.5%	1.53E−01	0.0084	0.9%	3.43E+04

Year	Year number	Discount rate	Present cost storm surge barrier (M€)	Rate of sea level rise (m/year)	Reduced discount rate	Present value flood damage (M€)
2093	82	5.5%	1.45E−01	0.0085	0.9%	3.43E+04
2094	83	5.5%	1.37E−01	0.0085	0.9%	3.44E+04
2095	84	5.5%	1.30E−01	0.0086	0.9%	3.45E+04
2096	85	5.5%	1.22E−01	0.0086	0.9%	3.46E+04
2097	86	5.5%	1.16E−01	0.0086	0.8%	3.47E+04
2098	87	5.5%	1.09E−01	0.0087	0.8%	3.48E+04
2099	88	5.5%	1.03E−01	0.0087	0.8%	3.50E+04
2100	89	5.5%	9.76E−02	0.0088	0.8%	3.51E+04
2101	90	5.5%	9.22E−02	0.0088	0.8%	3.52E+04
2102	91	5.5%	8.72E−02	0.0089	0.8%	3.54E+04
2103	92	5.5%	8.24E−02	0.0089	0.8%	3.56E+04
2104	93	5.5%	7.78E−02	0.0090	0.8%	3.57E+04
2105	94	5.5%	7.36E−02	0.0090	0.7%	3.59E+04
2106	95	5.5%	6.95E−02	0.0090	0.7%	3.61E+04
2107	96	5.5%	6.57E−02	0.0091	0.7%	3.63E+04
2108	97	5.5%	6.21E−02	0.0091	0.7%	3.66E+04
2109	98	5.5%	5.87E−02	0.0092	0.7%	3.68E+04
2110	99	5.5%	5.54E−02	0.0092	0.7%	3.70E+04
2111	100	5.5%	5.24E−02	0.0093	0.7%	3.73E+04
		Total	8.97E+02			4.22E+06